7-25-2007

Polarization control of direct (non-sequential) two-photon double ionization of He

Evgeny A. Pronin
University of Nebraska - Lincoln, epronin2@unl.edu

N. L. Manakov
Voronezh State University, manakov@phys.vsu.ru

S. I. Marmo
Voronezh State University

Anthony F. Starace
University of Nebraska-Lincoln, astarace1@unl.edu

Published in *Journal of Physics B: Atomic, Molecular and Optical Physics* **40** (2007), pp. 3115–3126; doi 10.1088/0953-4075/40/15/011 Online at http://stacks.iop.org/JPhysB/40/3115

Submitted April 27, 2007; revised June 26, 2007; published July 25, 2007

Polarization control of direct (non-sequential) two-photon double ionization of He

E. A. Pronin[1], N. L. Manakov[2], S. I. Marmo[2], and Anthony F. Starace[1]

[1] Department of Physics and Astronomy, University of Nebraska–Lincoln, Lincoln, NE 68588-0111, USA

[2] Department of Physics, Voronezh State University, Voronezh 394006, Russia

Abstract

An *ab initio* parametrization of the doubly-differential cross section (DDCS) for two-photon double ionization (TPDI) from an s^2 subshell of an atom in a $^1S_0$-state is presented. Analysis of the elliptic dichroism (ED) effect in the DDCS for TPDI of He and its comparison with the same effect in the concurrent process of sequential double ionization shows their qualitative and quantitative differences, thus providing a means to control and to distinguish sequential and non-sequential processes by measuring the relative ED parameter.

1. Introduction

Recent advances in the production of intense VUV and soft x-ray radiation have stimulated investigations of many electron photoprocesses in atoms owing to the possibility of obtaining new insights into electron correlations. The helium atom, the prototypical three-body Coulomb system, is the best candidate for such investigations. Over the past decade, electron correlations in single-photon double ionization of He by synchrotron radiation have been investigated in detail (see recent reviews [1] and references therein). At present, although the available intensities of VUV light sources are still in the perturbative regime (up to 10^{15} W cm^{-2}), these intensities allow probes of processes involving more than one photon [2]. Thus, many theoretical works have focused on two-photon double ionization (TPDI) of helium (see, e.g., [3–21]):

$$2\gamma + \mathrm{He} \rightarrow \mathrm{He}^{2+} + \mathrm{e}^- + \mathrm{e}^- . \text{ (‘d’)}$$

This direct (‘d’), or non-sequential, two-electron process occurs simultaneously with sequential (‘s’) processes. For photon energies E_γ less than the ionization potential of the He^+ ion (i.e., $E_\gamma < 2$ au), the ‘s’ process involves primarily the following two steps:

$$\gamma + \mathrm{He} \rightarrow \mathrm{He}^+ + \mathrm{e}^- , \qquad \text{(‘s1’)}$$

$$2\gamma + \mathrm{He}^+ \rightarrow \mathrm{He}^{2+} + \mathrm{e}^- . \qquad \text{(‘s2’)}$$

While the 'd' process is of second-order in the light intensity, I, the third-order (in I) 's' process is usually of comparable or greater magnitude for intensities that produce a measurable ionization yield, i.e., I of order 10^{14} W cm^{-2} [16]. We note that for the photon energies considered in this paper, there is another third-order sequential process that can lead to double ionization, but that, unlike the one we consider, involves electron correlation: specifically, two-photon single ionization of He with excitation of the residual ion to one of its excited states, $He^+(nl)$, followed by one-photon ionization of $He^+(nl)$. Owing to the necessity for electron correlation, the importance of this correlated third-order sequential process may be expected in general to be small compared to the uncorrelated sequential process we consider (cf figure 5 of [20]), although there may be particular photon frequencies at which it becomes significant.[3] However, in this paper we ignore this correlated sequential process.

Owing to the comparable or greater magnitude of the 's' process as compared to the 'd' process, one of the challenges in investigating the double ionization process either experimentally or computationally (by numerical solution of the time-dependent Schrödinger equation) is that of separating the 'd' (or TPDI) and 's' processes. However, there are ways to control the 's' and 'd' processes. One of them is proposed in [16], where the authors suggest enhancing the relative contribution of the 'd' channel by using an appropriate photon energy (e.g., $E_\gamma \sim 45$ eV) at which the cross section for the 's2' step of the 's' process has a broad local minimum [16].

In this work, we analyze the light polarization dependence of double ionization cross sections in the perturbative regime and discuss how to control and distinguish between the 'd' and 's' processes (even when they have comparable electron yields) by measuring the electron angular distributions for different light polarizations. For TPDI, it is most informative to measure the triply-differential cross section (TDCS), $\sigma_{\text{'d'}}^{(3)} \equiv \mathrm{d}^3\sigma_{\text{'d'}}/(\mathrm{d}E_2\mathrm{d}\Omega_1\mathrm{d}\Omega_2)$, where $\mathrm{d}\Omega_1$ and $\mathrm{d}\Omega_2$ are the ejection (solid) angles of the two photoelectrons, while E_2 is the energy of the second electron. An *ab initio* parametrization of the TDCS $\sigma_{\text{'d'}}^{(3)}$ has been obtained recently that is independent of the dynamical model describing electron correlations [22]. It shows that $\sigma_{\text{'d'}}^{(3)}$ exhibits a circular dichroism (CD) effect for the case of circularly polarized light (for both equal and non-equal energy sharing between the photoelectrons), whereas there is no CD effect for the 's' process. The observation of CD, however, requires coincidence measurements of the angular distributions of the two ionized electrons. In this work, we study the experimentally more feasible doubly-differential cross section (DDCS) for the 'd' process, analyze it both qualitatively and quantitatively (for He) and compare with the cross section for the 's2' process.

2. *Ab initio* parametrizations of DDCSs for the 'd' and 's' processes

2.1. Parametrization for the 'd' process

The DDCS for TPDI of an atom by radiation having an electric field vector $\mathbf{F}(\mathbf{r},t) = F\,\mathrm{Re}\,\{\mathbf{e}\exp[\mathrm{i}(\mathbf{k}\cdot\mathbf{r} - \omega t)]\}$ ($\mathbf{e}\cdot\mathbf{e}^* = 1$) and a photon flux density $|\mathbf{j}| = cF^2/(8\pi\hbar\omega)$ ($\mathrm{d}\sigma = \mathrm{d}W/|\mathbf{j}|^2$, where $\mathrm{d}W$ is the transition rate) is given in atomic units by

$$\mathrm{d}^2\sigma/(\mathrm{d}\Omega_2\,\mathrm{d}E_2) \equiv \sigma_{\text{'d'}}^{(2)} = \int \sigma_{\text{'d'}}^{(3)}\,\mathrm{d}\Omega_1 = \mathcal{A}\int |A_{\text{'d'}}|^2\,\mathrm{d}\Omega_1, \tag{1}$$

[3] For example, for circular light polarization, the two-photon ionization cross section of $He^+(1s)$ has zeros at frequencies $\omega_0^{(n,n+1)}$ in each frequency interval between pairs of neighboring resonances with $He^+(np)$ and $He^+((n+1)p)$ excited states. Thus, the correlated sequential process will be dominant at $\omega \approx \omega_0^{(n,n+1)}$. The lowest two values of $\omega_0^{(n,n+1)}$ are $\omega_0^{(2,3)} = 43.67$ eV and $\omega_0^{(3,4)} = 49.25$ eV.

where $\mathcal{A} = 8\pi^3 p_1 p_2/(c^2\omega^2)$,$p_i$ (i = 1, 2) are the photoelectron momenta and $E_i = p_i^2/2$. The amplitude $A_{\text{‘d’}}$ for a two-photon transition from an initial $s^2(^1S_0)$-state Φ_0 to the two electron continuum state $\Psi^{(-)}_{\mathbf{p}_1\mathbf{p}_2}$ involves the two-electron Green's function $G(E_0 + \omega)$,

$$A_{\text{‘d’}} = \left\langle \Psi^{(-)}_{\mathbf{p}_1\mathbf{p}_2} \middle| (\mathbf{e}\cdot\mathbf{D}) G(E_0+\omega) (\mathbf{e}\cdot\mathbf{D}) \middle| \Phi_0 \right\rangle, \tag{2}$$

where $(\mathbf{e}\cdot\mathbf{D}) = \mathbf{e}\cdot(\nabla_{\mathbf{r}_1} + \nabla_{\mathbf{r}_2})$ is the electric dipole operator (in velocity form) of the electron–photon interaction. Note also that $E_1 + E_2 = E_0 + 2\omega$.
Using expansions for $\Psi^{(-)}_{\mathbf{p}_1\mathbf{p}_2}$ and $G(E_0 + \omega)$ in bipolar harmonics $\mathrm{Y}^{l_1 l_2}_{LM}(\hat{\mathbf{r}}_1,\hat{\mathbf{r}}_2)$ [23], the evaluation of the angular integrals in (2) using the Wigner–Eckart theorem yields

$$A_{\text{‘d’}} = \sum_{L=0,2} \sum_{\substack{l_1 l_2 \\ s_1 s_2}} \frac{d^{s_1 s_2}_{l_1 l_2(L)}}{\sqrt{3(2L+1)}} \left(\{\mathbf{e}\otimes\mathbf{e}\}_L \cdot \mathrm{Y}^{l_1 l_2}_L(\hat{\mathbf{p}}_1, \hat{\mathbf{p}}_2) \right), \tag{3}$$

where

$$d^{s_1 s_2}_{l_1 l_2(L)} = \left\langle p_1 p_2 (l_1 l_2) L \middle|\middle| \mathbf{D} g_1^{s_1 s_2}(E_0+\omega)\mathbf{D} \middle|\middle| \Phi_0 \right\rangle \tag{4}$$

is the second-order two-electron reduced matrix element in which $\mathrm{g}_1^{s_1 s_2}(\mathcal{E})$ is the projection of the two-electron Green function $G(\mathcal{E})$ on the "intermediate" $^1P^o$ states of the electron pair (whose individual electron angular momenta are s_1 and s_2) and $|L(l_1 l_2)p_1 p_2\rangle$ is the L-wave component of the exact two-electron continuum state $\Psi^{(-)}_{\mathbf{p}_1\mathbf{p}_2}$ (whose individual angular momenta are l_1 and l_2). Owing to parity conservation, $s_1 + s_2$ = odd, and $l_1 + l_2$ = even. Further simplification of the bipolar harmonics $\mathrm{Y}^{l_1 l_2}_{LM}(\hat{\mathbf{p}}_1,\hat{\mathbf{p}}_2)$ in (3) (using the techniques developed in [24]) gives an *ab initio* parametrization for the TPDI amplitude $A_{\text{‘d’}}$ in terms of *four* polarization-independent dynamical amplitudes [22][4]. However, instead of using this invariant parametrization for $A_{\text{‘d’}}$ to obtain an invariant parametrization for the DDCS, it is simpler to substitute into the definition (1) the expression (3)for $A_{\text{‘d’}}$ and integrate over the angles of one of the electrons. As a result, we obtain

$$\sigma^{(2)}_{\text{‘d’}} = \sqrt{4\pi} \sum_{L=0,2} \sum_{L'=0,2} \sum_{g=0,2,4} B^{(\text{‘d’})}_{LL'g} \left(\{\{\mathbf{e}^*\otimes\mathbf{e}^*\}_{L'} \otimes \{\mathbf{e}\otimes\mathbf{e}\}_L\}_g \cdot \mathrm{Y}_g(\hat{\mathbf{p}}_2) \right), \tag{5}$$

where the dynamical factors $B^{(\text{‘d’})}_{LL'g}$ depend only on the electron energies E_1 and E_2,

$$B^{(\text{‘d’})}_{LL'g} = \frac{\mathcal{A}}{12\pi} \sum_{\substack{l_1 l_2 \\ s_1 s_2}} \sum_{\substack{l_1' l_2' \\ s_1' s_2'}} \delta_{l_1 l_1'} \sqrt{2l_2+1}\, C^{l_2' 0}_{l_2 0 g 0} \begin{Bmatrix} l_2 & L & l_1 \\ L' & l_2' & g \end{Bmatrix} d^{s_1 s_2}_{l_1 l_2(L)} \left[d^{s_1' s_2'}_{l_1' l_2'(L')} \right]^*, \tag{6}$$

and satisfy the following symmetry relation: $B^{(\text{‘d’})}_{LL'g} = [B^{(\text{‘d’})}_{LL'g}]^*$. Thus, the cross section $\sigma^{(2)}_{\text{‘d’}}$ involves six real dynamical parameters, e.g., $B^{(\text{‘d’})}_{000}$, Re $B^{(\text{‘d’})}_{202}$, Im $B^{(\text{‘d’})}_{202}$, and $B^{(\text{‘d’})}_{22g}$ with g = 0, 2, 4. The factors $B^{(\text{‘d’})}_{000}$ and $B^{(\text{‘d’})}_{22g}$ determine the contributions to $\sigma^{(2)}_{\text{‘d’}}$ originating respectively from ionization to the *S*-wave and *D*-wave channels of the two-electron continuum, while Re $B^{(\text{‘d’})}_{202}$ and Im $B^{(\text{‘d’})}_{202}$ describe the interference between the *S*-wave and *D*-wave contributions.

The spherical harmonic $\mathrm{Y}_{gq}(\hat{\mathbf{p}}_2)$ in (5) is the tensor product of g vectors $\hat{\mathbf{p}}_2$ [23]. Thus, using techniques for the reduction of tensors constructed from several vectors [25], the tensor product of **e**, **e***, and $\mathrm{Y}_{gq}(\hat{\mathbf{p}}_2)$ in (5) may be presented as a linear combination

[4] As shown in [22], the number of these amplitudes reduces to 3 for the cases of either equal energy sharing ($p_1 = p_2$) or circular light polarization ($|\zeta| \equiv |[\mathbf{e}^* \times \mathbf{e}]| = 1$; see the following main text) and, further, to 2 for $p_1 = p_2$ and $\xi = \pm 1$. (This latter fact has also been found in [19].)

of scalar products of the vectors involved. As a result, we obtain the following general parametrization for the TPDI DDCS:

$$\sigma^{(2)}_{\text{`d'}} = f_0^{(\text{`d'})} + f_1^{(\text{`d'})}|(\mathbf{e}\cdot\hat{\mathbf{p}}_2)|^2 + f_2^{(\text{`d'})}|(\mathbf{e}\cdot\hat{\mathbf{p}}_2)|^4 + \ell[\ell f_3^{(\text{`d'})} + f_4^{(\text{`d'})}\,\mathrm{Re}(\mathbf{e}\cdot\hat{\mathbf{p}}_2)^2 + f_5^{(\text{`d'})}\mathrm{Im}(\mathbf{e}\cdot\hat{\mathbf{p}}_2)^2\,], \quad (7)$$

where ℓ is the degree of linear light polarization ($\ell = (\mathbf{e}\cdot\mathbf{e})$, see below). The *six* polarization-invariant parameters $f_i^{(\text{`d'})}(p_1,p_2)$ depend only upon the photoelectron energies and can be expressed in terms of the dynamical factors $B^{(\text{`d'})}_{LL'g}$ as follows:

$$f_0^{(\text{`d'})} = \tfrac{1}{\sqrt{70}}\big(\sqrt{14}B_{220}^{(\text{`d'})} + 10B_{222}^{(\text{`d'})} + 3B_{224}^{(\text{`d'})}\big), \quad (8)$$

$$f_1^{(\text{`d'})} = -\tfrac{30}{\sqrt{70}}\big(B_{222}^{(\text{`d'})} + B_{224}^{(\text{`d'})}\big), \qquad f_2^{(\text{`d'})} = \tfrac{105}{2\sqrt{70}}B_{224}^{(\text{`d'})}, \quad (9)$$

$$f_3^{(\text{`d'})} = \tfrac{1}{3}\big[B_{000}^{(\text{`d'})} + \sqrt{10}\,\mathrm{Re}\,B_{202}^{(\text{`d'})} - \tfrac{1}{\sqrt{70}}\big(\sqrt{14}B_{220}^{(\text{`d'})} + 20B_{222}^{(\text{`d'})} - \tfrac{9}{2}B_{224}^{(\text{`d'})}\big)\big], \quad (10)$$

$$f_4^{(\text{`d'})} = -\sqrt{10}\,\mathrm{Re}\,B_{202}^{(\text{`d'})} + \tfrac{5}{\sqrt{70}}\big(4B_{222}^{(\text{`d'})} - 3B_{224}^{(\text{`d'})}\big), \qquad f_5^{(\text{`d'})} = \sqrt{10}\,\mathrm{Im}\,B_{202}^{(\text{`d'})}. \quad (11)$$

2.2. Parametrization for the 's' process

The 's1' step of the 's' process is described by its differential photoionization cross section, which is insensitive to the handedness of elliptically polarized light and has a well-known form in terms of the total cross section and an asymmetry parameter. As shown in [26], for the 's2' process, i.e., single-electron two-photon ionization, the differential cross section, $\mathrm{d}\sigma/\mathrm{d}\Omega \equiv \sigma_{\text{`s2'}}$, has the same six-parameter form as in (7) for the general case of non-zero angular momentum l of an initially-bound electron (because the same set of vectors (**e**, **e***, and $\hat{\mathbf{p}}$) occurs in both problems). For ionization from an *s*-state (e.g., $He^+(1s)$), $\sigma_{\text{`s2'}}$ simplifies, since for this case the amplitude $A_{\text{`s2'}}$ is a scalar that involves only two terms, which are proportional to $(\mathbf{e}\cdot\hat{\mathbf{p}})^2$ and ℓ (cf [26]),

$$A_{\text{`s2'}} = \sum_{l=0,2} A_l(p)(\{\mathbf{e}\otimes\mathbf{e}\}_l \cdot \mathrm{Y}_l(\hat{\mathbf{p}})) = \frac{1}{\sqrt{24\pi}}[3\sqrt{5}A_2(p)(\mathbf{e}\cdot\hat{\mathbf{p}})^2 - (\sqrt{2}A_0(p) + \sqrt{5}A_2(p))\ell], \quad (12)$$

where

$$A_l(p) = \frac{2\pi}{p}(-i)^l \mathrm{e}^{\mathrm{i}\delta_l(p)}\frac{d_l(p)}{\sqrt{3(2l+1)}}, \qquad p = \sqrt{2(E_{1s}+2\omega)}, \quad (13)$$

$\delta_l(p)$ is the Coulomb scattering phase and $d_l(p) \equiv \langle R_{pl}\|\nabla_1 g_1(E_{1s}+\omega)\nabla_1\|R_{1s}\rangle$ is the reduced matrix element for two-photon ionization in which $g_1(E_{1s}+\omega)$ is the radial part of the Coulomb Green's function. The resulting expression for $\sigma_{\text{`s2'}}$,

$$\mathrm{d}\sigma/\mathrm{d}\Omega \equiv \sigma_{\text{`s2'}} = \mathcal{B}|A_{\text{`s2'}}|^2, \quad \mathcal{B} = p/(c^2\omega^2), \quad (14)$$

may be presented in a form similar to (5),

$$\sigma_{\text{`s2'}} = \sqrt{4\pi}\sum_{l=0,2}\sum_{l'=0,2}\sum_{g=0,2,4} B^{(\text{`s2'})}_{ll'g}(\{\{\mathbf{e}^*\otimes\mathbf{e}^*\}_{l'}\otimes\{\mathbf{e}\otimes\mathbf{e}\}_l\}_g \cdot \mathrm{Y}_g(\hat{\mathbf{p}})), \quad (15)$$

where the dynamical factors B have much simpler forms than those for the 'd' process:

$$B^{(\text{`s2'})}_{ll'g} = \frac{1}{4\pi}\mathcal{B}A_l(p)A^*_{l'}(p)\sqrt{2l+1}C^{l'0}_{l0g0}, \qquad B^{(\text{`s2'})}_{ll'g} = \big[B^{(\text{`s2'})}_{l'lg}\big]^*. \quad (16)$$

Owing to the similarity between expressions (5) and (15), the invariant parametrization of $\sigma_{\text{`s2'}}$ also has the form (7) (substituting there $\mathbf{p}_2 \rightarrow \mathbf{p}$), except that $f_0^{(\text{`s2'})}$ and $f_1^{(\text{`s2'})}$ vanish. The explicit forms for the remaining invariant parameters, $f_2^{(\text{`s2'})} - f_5^{(\text{`s2'})}$, follow from (9)–(11) on making the replacement $B^{(\text{`d'})}_{LL'g} \rightarrow B^{(\text{`s2'})}_{ll'g}$. Thus, the angular distribution for two-photon ionization of $He^+(1s)$ is parametrized by four dynamical factors, $f_i^{(\text{`s2'})}(i = 2, ..., 5)$, independent of the light polarization and photoelectron ejection angle. Also, the differences in the ejected electron energies (which are fixed in the 's' process, but are shared between the two electrons in the 'd' process) as well as in the physical mechanisms for electron ejection between the 's' and 'd' processes ensure pronounced differences in the magnitudes of polarization effects in these processes, thus providing a means to control the 'd' process contribution.

2.3. Alternative parametrization exhibiting the elliptic dichroism effect

To separate explicitly the polarization and angular dependences in (7), whose form applies to both the 'd' and 's2' cross sections, we parametrize the photon polarization vector as $\mathbf{e} = (\hat{\epsilon} + i\eta\hat{\zeta})/(1 + \eta^2)^{1/2}$ $(-1 \leq \eta \leq 1)$, where $\hat{\zeta} = [\hat{\mathbf{k}} \times \hat{\epsilon}]$, and $\hat{\epsilon}$ and $\hat{\mathbf{k}}$ indicate the directions of the major axis of the polarization ellipse and the photon wave vector $\mathbf{k}$. The ellipticity η is related to the degrees of linear and circular polarization, ℓ and ξ: $\ell = (1 - \eta^2)/(1 + \eta^2) = (\mathbf{e} \cdot \mathbf{e})$, $\xi = 2\eta/(1 + \eta^2) = i(\hat{\mathbf{k}} \cdot [\mathbf{e}^* \times \mathbf{e}])$; $0 \leq \ell \leq 1$, $-1 \leq \xi \leq +1$, $\ell^2 + \xi^2 = 1$. With these definitions and parametrization (7), the cross sections $\sigma_{\text{`d'}}^{(2)}$ and $\sigma_{\text{`s2'}}$ both have the following form (where, here and in (18)–(20), we omit any additional indices since these equations are valid for both the 'd' and 's2' processes):

$$\sigma = \sigma_0 + \xi\ell\sigma_{\text{ED}}, \tag{17}$$

where σ_0 is invariant to $\mathbf{e} \rightarrow \mathbf{e}^*$ (i.e., to a change in the sign of ξ), while the term $\xi\ell\sigma_{\text{ED}}$ is *dichroi*c (i.e., it changes sign when $\xi \rightarrow -\xi$). The dichroic term in (17) vanishes for purely circular polarization ($\xi = \pm 1$, $\ell = 0$) and describes the elliptic dichroism (ED) effect; it is maximal for $\ell = |\xi| = 2^{-1/2}$. The general expressions for σ_0 and σ_{ED} in (17) havethe following forms (cf [26]):

$$\begin{aligned}\sigma_0 = f_0 + f_1[\ell(\hat{\boldsymbol{\epsilon}} \cdot \hat{\mathbf{p}})^2 + [\hat{\mathbf{k}} \times \hat{\mathbf{p}}]^2(1 - \ell)/2] + f_2[\ell(\hat{\boldsymbol{\epsilon}} \cdot \hat{\mathbf{p}})^2 + [\hat{\mathbf{k}} \times \hat{\mathbf{p}}]^2(1 - \ell)/2]^2 \\ + \ell\{\ell f_3 + f_4[(\hat{\boldsymbol{\epsilon}} \cdot \hat{\mathbf{p}})^2 - [\hat{\mathbf{k}} \times \hat{\mathbf{p}}]^2(1 - \ell)/2]\},\end{aligned} \tag{18}$$

$$\sigma_{\text{ED}} = f_5(\hat{\boldsymbol{\epsilon}} \cdot \hat{\mathbf{p}})(\hat{\boldsymbol{\zeta}} \cdot \hat{\mathbf{p}}) = f_5(\hat{\boldsymbol{\epsilon}} \cdot \hat{\mathbf{p}})(\hat{\boldsymbol{\epsilon}} \cdot [\hat{\mathbf{k}} \times \hat{\mathbf{p}}]) = f_5 \sin^2\theta \sin\varphi \cos\varphi, \tag{19}$$

where (θ, φ) are the spherical angles of the vector $\mathbf{p}$ in the reference frame $\{\hat{\boldsymbol{\epsilon}}, \hat{\boldsymbol{\zeta}}, \hat{\mathbf{k}}\}$.(Note that f_0 and f_1 in (18) vanish for the case of the 's2' process for $He^+(1s)$.)

Expressions (17)–(19) give an alternative parametrization to (7) for the DDCS in terms of real vectors.[5] The ED term, σ_{ED}, involves only the parameter f_5, while σ_0 involves all others. From the explicit forms (11) for f_5 and (6) and (16) for B_{202} $(= B^*_{022})$, one sees that the ED effect in both the 'd' and 's' processes originates from the interference between real and imaginary parts of polarization-invariant components of the generally non-Hermitian transition amplitudes to the *S*-wave ($L = 0$, or $l = 0$) and *D*-wave ($L = 2$, or $l = 2$) continuum channels, in agreement with general arguments [27] on the origin of dichroic effects in photoprocesses involving unpolarized atoms. Another peculiarity of the ED term (19) is its linear dependence on $\sin\varphi$ (compared to the $\sin^2\varphi$-dependence of the term σ_0), which causes an asymmetry in the angular distributions for elliptically polarized light when φ

[5] An alternative representation for σ_0 in (18) in terms of $(\hat{\boldsymbol{\epsilon}} \cdot \hat{\mathbf{p}})^2$ and $(\hat{\boldsymbol{\zeta}} \cdot \hat{\mathbf{p}})^2$ may be obtained using the identity: $[\hat{\mathbf{k}} \times \hat{\mathbf{p}}]^2 = (\hat{\boldsymbol{\epsilon}} \cdot \hat{\mathbf{p}})^2 + (\hat{\boldsymbol{\zeta}} \cdot \hat{\mathbf{p}})^2$.

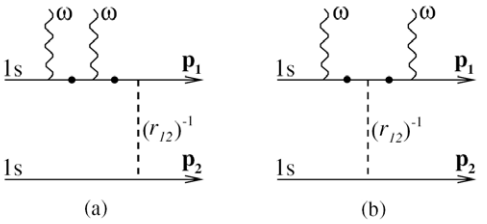

Figure 1. Schematic diagrams for knock-out contributions to the TPDI transition amplitude with both photons absorbed by one electron. Solid dots indicate summations over intermediate states. Diagrams with interchanged $\mathbf{p}_1$ and $\mathbf{p}_2$ must also be included.

$\rightarrow -\varphi$. Finally, we note that $\sigma^{(2)}_{\text{`d'}}$ is described by a set of only three parameters for either linear or circular polarization (so that the angular distributions are axially symmetric about either $\hat{\boldsymbol{\epsilon}}$ or $\mathbf{k}$, respectively). Thus, only the use of elliptically polarized light allows one to measure the entire set of six independent invariant parameters, $f_i^{(\text{`d'})}$, that completely describe the TPDI DDCS.

3. Results for He

3.1. Numerical method and measurement geometries

The above parametrizations for the DDCSs (and, in particular, the ED contributions to the DDCSs) are exact and valid for any dynamical model describing electron correlations. In order to estimate the magnitude of the ED effect in TPDI of He, we describe electron correlations using the approach of [22], i.e., the lowest-order perturbation theory (LOPT) in the interelectron interaction $1/r_{12}$. Moreover, we consider only those two contributions associated with the knock-out mechanism in which both photons are absorbed by the same electron (see Figure 1). As shown in [28], the knock-out mechanism is the dominant one in single-photon double ionization for excess energies of the order of tens of eV. Also, more accurate numerical analyses [18, 20] exhibit the dominant role of final state correlations in TPDI. Consistent with those results, our calculations indicate that the "intermediate state correlation" diagram in Figure 1(b) gives a negligible contribution compared to that of the final state correlation diagram in Figure 1(a). Besides the diagrams shown in Figure 1, there are also three LOPT diagrams that correspond to absorption of a single photon by each of the two electrons. As discussed in [22] for one of the photon energies considered in this paper (~45 eV) and non-equal energy sharing between the photoelectrons, the contributions of these diagrams are largest in a narrow interval of nearly equal escape angles of the two electrons, but outside this region of small mutual angles are as much as two to three orders of magnitude smaller. In addition, one of these diagrams (corresponding to final state correlation) becomes divergent as $1/|E_1 - E_2|$ in the vicinity of equal energy sharing ($E_1 = E_2$), while the two other diagrams are finite and their contribution is small (compared to that of the final state knock-out diagram) for any energy sharing and any mutual angle. Thus, in order to obtain correct results it is necessary to include high-order effects in $1/r_{12}$ and/or carry out a renormalization of the singular diagram to compensate the formal divergence of the LOPT result for this diagram. Owing to these difficulties with this latter diagram, we estimate the magnitudes of the analytically predicted effects in this paper based on the knock-out diagrams in Figure 1, which give magnitudes of the total TPDI cross sections comparable to those predicted by the *R* matrix approach [11].

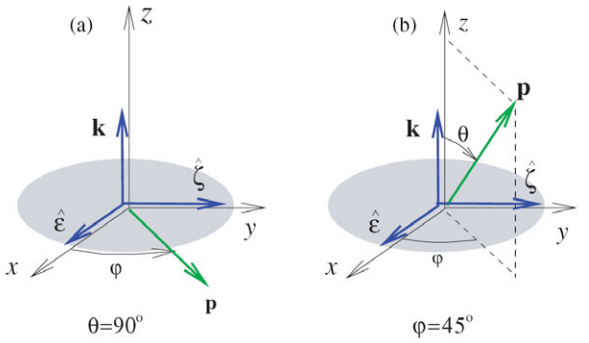

Figure 2. Two measurement geometries in which the ED effect is maximal in the 'd'- and 's'-channels for double ionization of He: **(a)** $\theta = 90°$ is fixed, φ is varied; **(b)** $\varphi = 45°$ is fixed, θ is varied.

To calculate matrix elements for two-photon ionization of $He^+(1s)$, we use the generalized Sturmian expansion of the Coulomb Green's function [29], which allows an analytic evaluation of the matrix element $d_l(p)$ in (13) in terms of a convergent series. Thus, our results for $\sigma_{\text{'s2'}}$ and the ED effect for the 's' process are exact.

In Figures 2(a) and (b), we present two geometries in which the ED effect is maximal. These involve respectively measurements in the plane orthogonal to the wave vector k (a) and in the plane involving the vector **k** located at an angle of 45° with respect to the major and minor axes of the polarization ellipse (b). To describe the ED effect, we define the relative ED parameter,

$$\delta_{\text{ED}} \equiv \frac{\sigma(\xi) - \sigma(-\xi)}{\sigma(\xi) + \sigma(-\xi)} = \xi \ell \frac{\sigma_{\text{ED}}}{\sigma_0}. \tag{20}$$

Since the φ and θ dependences of δ_{ED} in the intervals (0, 180°) and (180°, 360°) are the same, we only present results for the interval (0, 180°). Also in Figures 3, 5, and 6, we present the cross section for the 'd' process integrated over the electron energies,

$$\sigma_{\text{'d'}}^{(1)} \equiv \int_0^{E/2} \sigma_{\text{'d'}}^{(2)}\, \mathrm{d}E_2, \tag{21}$$

since for this case there is no need to detect the electron energy and we expect that this type of measurement may be the most feasible experimentally.

3.2. Results for Eγ = 45 eV

In Figures 3(a) and (b), we present results for the geometry in Figure 2(a) for a photon energy $E_\gamma = 45$ eV, which corresponds to the 29th harmonic of a Ti:sapphire laser ($\lambda = 800$ nm). One sees that the DDCS of TPDI (cf Figure 3(a)) exhibits a pronounced ED effect. The relative ED parameter (cf Figure 3(a)) approaches its maximum magnitude at $\varphi = 52°$ and 128°, $\xi = 2^{-1/2}$, where $|\delta_{\text{ED}}^{\text{'d'}}| = 12.2\%$. The zeros of δ_{ED} at $\varphi = \pi n$ ($n = 0, 1, 2$) have a geometrical origin, as may be verified from expression (19) for σ_{ED}. For the 's2' process (cf Figures 3(b) and (b)), the positions of the zeros of δ_{ED} are the same, but the behavior of δ_{ED} near the maxima is quite different. The maxima have almost the same positions as in Figure 3(a′), $\varphi = 53°$ and 127°, but the maximum value $|\delta_{\text{ED}}| = 100\%$ is approached at $\xi = 0.38$. The dichroic effect is huge because $\sigma_0^{\text{'s2'}}$ has a minimum for these angles and ξ, so that the term $|\ell\xi\sigma_{\text{ED}}|$ becomes almost equal to σ_0. For these cases (i.e., $\varphi = 53°$, $\xi = 0.38$, and $\varphi = 127°$, $\xi = -0.38$), the 's2' process is suppressed by three orders of magnitude.

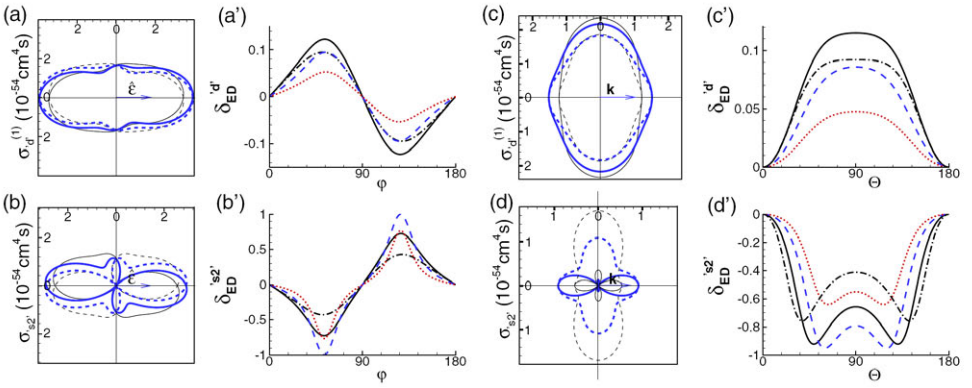

Figure 3. Cross sections σ and relative ED parameters δ_{ED} for the 'd'-channel ((a), (a′) and (c), (c′)) and the 's2'-channel ((b), (b′) and (d), (d′)) of double ionization of He by photons of energy E_γ = 45 eV for the geometries in Figure 2(a) ((a), (a′) and (b), (b′)) and Figure 2(b) ((c), (c′) and (d), (d′)). In Figures (a), (b) and (c), (d): black thin solid and dashed lines stand for $\xi = 2^{-1/2}$ and $\xi = -2^{-1/2}$; blue thick solid and dashed lines stand for $\xi = 0.38$ and $\xi = -0.38$. In Figures (a′), (b′), and (c′), (d′): black dot-dashed lines stand for $\xi = 0.88$; solid black lines stand for $\xi = 2^{-1/2}$; dashed blue lines stand for $\xi = 0.38$; dotted red lines stand for $\xi = 0.20$.

In general, even if the ED effect is significant in only one of the 's' or 'd' processes, it is possible to distinguish these processes experimentally from information on the magnitudes of $\delta_{ED}^{\text{'s2'}}$ and $\delta_{ED}^{\text{'d'}}$. Note first that $\delta_{ED}^{\text{'s'}} = \delta_{ED}^{\text{'s2'}}$, since there are no dichroic effects in the 's1' step of the 's' process. Furthermore, the total (measured) relative ED parameter for double ionization, which involves both the 's' and 'd' processes, may be expressed as $\delta_{ED}^{\text{'s'+'d'}} = (1-x)\,\delta_{ED}^{\text{'s'}} + x\,\delta_{ED}^{\text{'d'}}$, where $x \equiv (\sigma^{\text{'d'}}(\xi) + \sigma^{\text{'d'}}(-\xi))\,/(\sigma^{\text{'s'+'d'}}(\xi) + \sigma^{\text{'s'+'d'}}(-\xi))$ is the relative contribution of the 'd' process. An experimental measurement of $\delta_{ED}^{\text{'s2'+'d'}}$ at particular values of φ and ξ combined with our predicted values of $\delta_{ED}^{\text{'s'}}$ and $\delta_{ED}^{\text{'d'}}$ from Figures 3(b′) and (a′) allows a determination of the value of x, the fraction of measured electrons produced through the 'd'-channel (with $(1 - x)$ produced through the 's'-channel). Of course, if the ED effect is small in both the 's' and 'd' processes, then it may be difficult to measure $\delta_{ED}^{\text{'s'+'d'}}$, which will also be small.

In Figures 3(c), (c′) and (d), (d′) for the geometry in Figure 2(b), one sees even more distinctive features in the cross sections and relative ED parameters for 'd' and 's2' processes. For the 'd' process, δ_{ED} has a maximum at $\theta = 90°$ for any ξ . (The absolute maximum is $|\,\delta_{ED}\,| = 11.5\%$ at $\xi = 2^{-1/2}$). For the 's2' process, however, the positions of the maxima depend on ξ .For $\xi = 0.88$, the maximum is at $\theta = 38°, 142°$; for $\xi = 2^{-1/2} = 0.71$ at $\theta = 49°, 131°$; for $\xi = 0.38$ at $\theta = 60°, 120°$ and for $\xi = 0.20$ at $\theta = 63°, 117°$. Note that $\delta_{ED}^{\text{'s'}} = -92.2\%$ and $\delta_{ED}^{\text{'d'}} = 9.2\%$ for $\theta = 49°, \xi = 2^{-1/2}$.

In Figure 4, we present the DDCS $\sigma_{\text{'d'}}^{(2)}$ for two fixed energy sharings between the electrons: (5.5 + 5.5) eV and (9.9 + 1.1) eV. The results for equal energy sharing are similar to those for the energy-integrated DDCS $\sigma_{\text{'d'}}^{(1)}$ in Figure 3. For both geometries in Figure 2, the ED effect is more pronounced for unequal energy sharing: the maximum of $|\delta_{ED}|$ is 18.5% for this case, while $|\delta_{ED}|_{max} = 5.9\%$ for equal sharing.

3.3. Results for E_γ = 41.8 eV and 48 eV

In Figures 5 and 6, the cross sections $\sigma_{\text{'d'}}^{(1)}$ and $\sigma_{\text{'s2'}}$ for the 'd' and 's2' processes are shown for photon energies E_γ = 41.8 eV and 48 eV, which correspond to the 27th and 31st

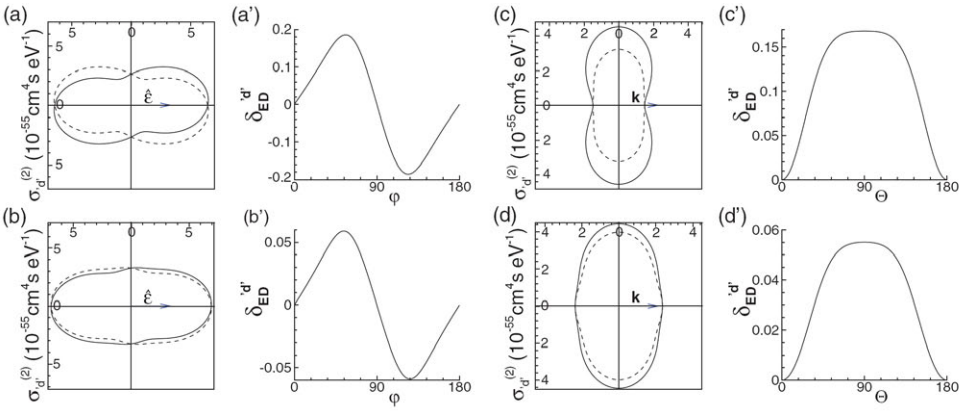

Figure 4. DDCS $\sigma_{\text{'d'}}^{(2)}$ and the relative ED parameter for TPDI of He by a 45 eV photon for energy sharings (9.9 + 1.1) eV ((a), (a′) and (c), (c′)) and (5.5 + 5.5) eV ((b), (b′) and (d), (d′)) for the geometries in Figure 2(a) ((a), (a′), (b), (b′)) and in Figure 2(b) ((c), (c′), (d), (d′)). Solid lines: $\xi = 2^{-1/2}$; dashed lines: $\xi = -2^{-1/2}$.

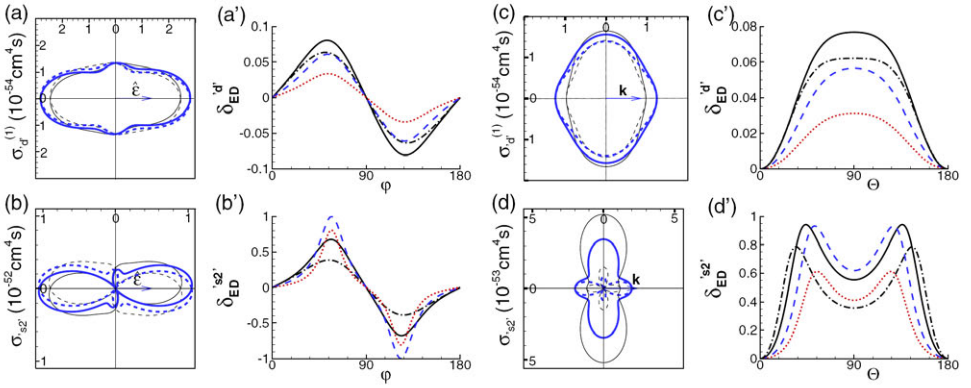

Figure 5. Same as Figure 3, but for the photon energy E_γ = 41.8 eV.

harmonics of a Ti:sapphire laser (λ = 800 nm). Compared to the case of E_γ = 45 eV, $\sigma_{\text{'s2'}}$ is more than an order of magnitude larger for E_γ = 41.8 eV and 48 eV, so that $E\gamma$ = 45 eV is indeed preferable for observations of the 'd' process, in agreement with the results in [16]. Another distinct feature of the 's2' process is that the sign of the relative ED parameter $\delta_{\text{ED}}^{\text{'s'}}$ at 41.8 eV and 48 eV differs from that for 45 eV. Concerning the 'd' process, one sees that the ED effect for this process is more pronounced at higher E_γ .

4. Summary and discussion

In this paper, we have provided exact parametrizations of the DDCS for TPDI from an s^2 subshell of an atom in a $^1S_0$-state. We have also given a similar, exact parametrization of the cross section for the dominant sequential ionization process, which requires at least three photons for photon energies below the ionization threshold of the ground state of the

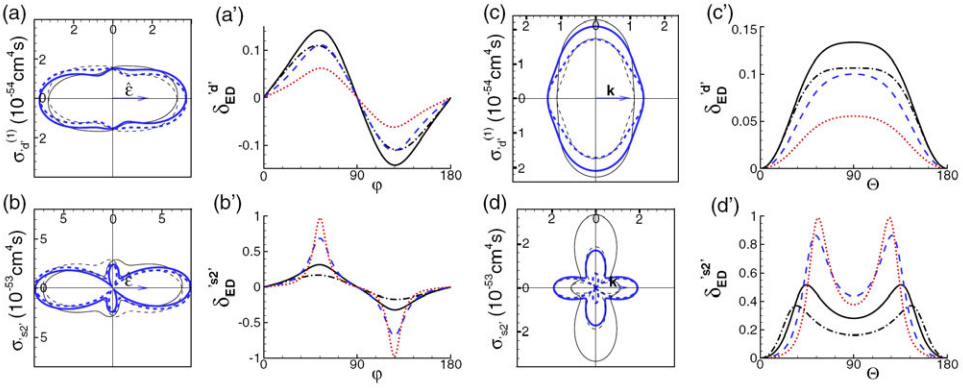

Figure 6. Same as Figure 3, but for the photon energy E_γ = *48 eV.*

singly-ionized atom. Furthermore, we have provided in addition exact parametrizations of the dichroism effects that may be observed in the cross section by either the direct or the sequential process. For the two measurement geometries (cf Figures 2(a) and (b)) for which these dichroic effects are predicted to be maximal, we have estimated their magnitudes for the case of He for three different photon energies.

Our numerical estimates for He show that the 'd' and 's' processes give very different elliptic dichroism results. In particular, as shown in Figure 3, the relative ED parameters for the 'd' and 's' processes have opposite signs for the parameters considered. Furthermore, for a photon energy of 45 eV and the measurement geometry in Figure 2(a), the maximal values of the dichroism parameter resulting from the 's' process occur for electron ejection angles at which the cross section for the 's' process decreases by three orders of magnitude, whereas there is no such drop in the value of the cross section at these same ejection angles for the 'd' process. Thus, this photon energy and this measurement geometry appear to be optimal for distinguishing the dichroic effects of the 'd' process from those resulting from the 's' process.

In general, in order for experiment to distinguish the 'd' and 's' processes, a coincidence measurement of the two electron energies must be made, from which comparison with our parametrization and estimates for the TDCS [22] can be made. In cases in which the coincidence energy measurements are not possible, measurements of the dichroic effects predicted in this paper for the DDCS can be made. In this case, both the 'd' and 's' processes will contribute to the measurement (or to the result of a direct solution of the time-dependent Schrödinger equation). In this case, we have sketched in section 3.2 how experimental measurements of the ED parameter for the case in which both the 'd' and 's' processes contribute to the measurement together with theoretical predictions for the separate ED parameters for the 'd' and 's' processes may be used to predict the relative contribution of the 'd' process to the double ionization yield. We note that since the relative ED parameters involve the ratios of cross sections, results of calculations of these parameters may be expected to be less sensitive to the theoretical models used than the cross sections themselves.

As shown in this paper (cf (17) and (19)), the predicted dichroic effects in the DDCS depend upon a single, polarization-independent parameter f_5. Moreover, this parameter is sensitive to interference between S and D channels of the two-photon double ionization process (cf (11)). It thus provides a very sensitive test of the accuracy of theoretical models. We note that its value for the 'd' process alone may be determined by experiments that measure this parameter in the presence of both the 'd' and 's' processes. The reason is that

f_5 may be calculated exactly for the 's' process since it originates only from the 's2' process for a hydrogen-like system. For the three photon energies considered in this paper (i.e., 41.8 eV, 45 eV, and 48 eV), $f_5^{(\text{'s2'})}$ takes the values -0.7424×10^{-52}, 0.2708×10^{-53}, and -0.2930×10^{-52} cm^4 s, respectively. Thus, if an experiment measures $f_5^{(\text{'d'+'s2'})}$, then $f_5^{(\text{'d'})} = f_5^{(\text{'d'+'s2'})} - f_5^{(\text{'s2'})}$.

Finally, we note that the magnitudes of $\sigma_{\text{'d'}}^{(1)}$ at 45 eV and 48 eV are almost equal and slightly larger than at 41.8 eV, in qualitative agreement with the behavior of the TPDI total cross section $\sigma_{\text{'d'}}^{(0)}(\omega)$ found in [18, 20, 21] for the case of linear polarization. For elliptical polarization, our general parametrization of the total cross section is

$$\sigma_{\text{'d'}}^{(0)}(\omega;\ell) = \int \sigma_{\text{'d'}}^{(2)}\,\mathrm{d}E_2\,\mathrm{d}\Omega_2 = \frac{4\pi}{3}\left[\ell^2 \tilde{B}_{000}^{(\text{'d'})} + \frac{1}{\sqrt{5}}(3-\ell^2)\tilde{B}_{220}^{(\text{'d'})}\right], \tag{22}$$

where the factors $\tilde{B}_{LL0}^{(\text{'d'})}$,

$$\tilde{B}_{LL0}^{(\text{'d'})} = \int_0^{E/2} B_{LL0}^{(\text{'d'})}\,\mathrm{d}E_2,$$

determine the TPDI partial cross sections corresponding to the *S*-wave ($L = 0$) and /*D*-wave ($L = 2$) continuum channels. (In particular, for $\omega = 41.8$, 45, and 48 eV, the ratio $\tilde{B}_{000}^{(\text{'d'})}/\tilde{B}_{220}^{(\text{'d'})}$ is 0.82, 0.73, and 0.69, respectively.) For the case of linear polarization and $\omega = 41.8$ eV, our result for $\sigma_{\text{'d'}}^{(0)}$ is 1.9×10^{-53} cm^4 s, which is close to the *R* matrix result [11], about three times less than the recent results of [21] and about an order of magnitude less than the recent results of [18]. (Note also our results $\sigma_{\text{'d'}}^{(0)} = 2.5 \times 10^{-53}$ and 2.4×10^{-53} cm^4 s for $\omega =$ 45 and 48 eV, respectively.) Thus, in using our numerical results for $\sigma_{\text{'d'}}^{(1)}$ and $\sigma_{\text{'d'}}^{(2)}$ in Figures 3–6 to estimate whether experimental measurements are feasible, it may be reasonable to scale our estimates upward by up to an order of magnitude. We emphasize, however, that our general parametrizations (7), (17)–(19) for the TPDI DDCS are independent of any particular dynamical model. Thus, more accurate numerical calculations of the matrix elements $d_{l_1 l_2 (L)}^{s_1 s_2}$ in (6) and hence the parameters $f_i^{(\text{'d'})}$ in (8)–(11) may be employed in this parametrization to obtain the absolute magnitudes of the TPDI cross sections. We reiterate, however, that the relative magnitudes of the ED effects predicted here may be expected to be much less sensitive to the numerical approach employed.

Acknowledgments

This work was supported in part by National Science Foundation Grant PHY-0601196, by Russian Foundation for Basic Research Grant 07-02-00574 and by CRDF & BRHE Grant BP2M10.

References

[1] Briggs J S and Schmidt V 2000 *J. Phys. B: At. Mol. Opt. Phys.* **33** R1
Avaldi L and Huetz A 2005 *J. Phys. B: At. Mol. Opt. Phys.* **38** S861

[2] Nabekawa Y, Hasegawa H, Takahashi E J, and Midorikawa K 2005 *Phys. Rev. Lett.* **94** 043001
Hasegawa H, Takahashi E J, Nabekawa Y, Ishikawa K L, and Midorikawa K 2005 *Phys. Rev. A* **71** 023407

[3] Pindzola M S and Robicheaux F 1998 *J. Phys. B: At. Mol. Opt. Phys.* **31** L823

[4] Kornberg M A and Lambropoulos P 1999 *J. Phys. B: At. Mol. Opt. Phys*. **32** L603

[5] Parker J S, Moore L R, Meharg K J, Dundas D, and Taylor K T 2001 *J. Phys. B: At. Mol. Opt. Phys.* **34** L69

[6] Nikolopoulos L A A and Lambropoulos P 2001 *J. Phys. B: At. Mol. Opt. Phys.* **34** 545

[7] Mercouris T, Haritos C, and Nicolaides C A 2001 *J. Phys. B: At. Mol. Opt. Phys.* **34** 3789

[8] Colgan J and Pindzola M S 2002 *Phys. Rev. Lett.* **88** 173002

[9] Laulan S and Bachau H 2003 *Phys. Rev. A* **68** 013409

[10] Piraux B, Bauer J, Laulan S, and Bachau H 2003 *Eur. Phys. J. D* **26** 7

[11] Feng L and van der Hart H W 2003 *J. Phys. B: At. Mol. Opt. Phys.* **36** L1

[12] Taylor K T, Parker J S, Dundas D, Meharg K J, Doherty B J S, Murphy D S, and McCann J F 2005 *J. Electron Spectrosc. Relat. Phenom.* **144** 1191

[13] Hu S X, Colgan J, and Collins L A 2005 *J. Phys. B: At. Mol. Opt. Phys.* **38** L35

[14] Lambropoulos P, Nikolopoulos L A A, and Makris M G 2005 *Phys. Rev. A* **72** 013410

[15] Barna I F, Wang J, and Burgdörfer J 2006 *Phys. Rev. A* **73** 023402

[16] Nikolopoulos L A A and Lambropoulos P 2006 *J. Phys. B: At. Mol. Opt. Phys.* **39** 883

[17] Kheifets A S and Ivanov I A 2006 *J. Phys. B: At. Mol. Opt. Phys.* **39** 1731

[18] Foumouo E, Lagmago Kamta G, Edah G, and Piraux B 2006 *Phys. Rev. A* **74** 063409

[19] Kheifets A S, Ivanov I A, and Bray I 2007 *Phys. Rev. A* **75** 024702

[20] Nikolopoulos L A A and Lambropoulos P 2007 *J. Phys. B: At. Mol. Opt. Phys.* **40** 1347

[21] Ivanov I A and Kheifets A S 2007 *Phys. Rev.* A **75** 033411

[22] Istomin A Y, Pronin E A, Manakov N L, and Starace A F 2006 *Phys. Rev. Lett.* **97** 123002

[23] Varshalovich D A, Moskalev A N, and Khersonskii V K 1988 *Quantum Theory of Angular Momentum* (Singapore: World Scientific)

[24] Manakov N L, Marmo S I, and Meremianin A V 1996 *J. Phys. B: At. Mol. Opt. Phys.* **29** 2711

[25] Manakov N L and Merem'yanin A V 1997 *Zh. Eksp. Teor. Fiz.* **112** 1984
Manakov N L and Merem'yanin A V 1997 *Sov. Phys.–JETP* **84** 1080 (Engl. Transl.)

[26] Manakov N L, Maquet A, Marmo S I, Veniard V, and Ferrante G 1999 *J. Phys. B: At. Mol. Opt. Phys.* **32** 3747

[27] Manakov N L, Frolov M V, Borca B, and Starace A F 2003 *J. Phys. B: At. Mol. Opt. Phys.* **36** R49, section 1.1

[28] Istomin A Y, Manakov N L, and Starace A F 2002 *J. Phys. B: At. Mol. Opt. Phys.* **35** L543
Istomin A Y, Manakov N L, and Starace A F 2004 *Phys. Rev. A* **69** 032713

[29] Krylovetsky A A, Manakov N L, and Marmo S I 2001 *Zh. Eksp. Teor. Fiz.* **119** 45
Krylovetsky A A, Manakov N L, and Marmo S I 2001 *Sov. Phys.—JETP* **92** 37 (Engl. Transl.)